

# Development of Thin Film Silicon Solar Cells Below 100°C on Flexible Low Cost Substrates

P.C.P. Bronsveld, J.K. Rath\* and R.E.I. Schropp  
Utrecht University, Debye Institute, SID – Physics of devices  
P.O. Box 80.000, 3508 TA Utrecht, the Netherlands  
Phone: +31 (0)30 2532 964 Fax: +31 (0)30 2543 165  
E-mail: [p.c.p.bronsveld@phys.uu.nl](mailto:p.c.p.bronsveld@phys.uu.nl)

**Abstract**— Several series of silicon thin films deposited at different substrate temperatures at and below 100°C, were characterized with respect to their, electrical, structural and optical properties. Based on the knowledge gained, doped layers and solar cells were designed and deposited at substrate temperatures of 39°C and 100°C. Promising results were obtained for a working solar cell at 39°C. Further, the 39°C layers proved to be good model material to get a better understanding of the growth of microcrystalline material, which might also be applicable for layers made at higher temperatures. At 100°C we obtained good results for a cell on a textured superstrate: a conversion efficiency of 7.2 %, which is to our knowledge the highest efficiency reported for thin film silicon at this substrate temperature. On Indium Tin Oxide (ITO) coated Polyethylene Terephthalate (PET), there are still some technical issues to overcome.

**Keywords**— solar cells; flexible substrates; low cost; amorphous silicon; low temperature deposition

## I. INTRODUCTION

Fabrication of solar cells on thin and flexible foil has advantages on both the production and the fabrication side. These flexible products can be applied in consumer products and in building integration. Current technologies to achieve flexibility normally include several processing steps like slicing or polishing down of wafers, etching of sacrificial superstrates or adaptation of plastics to make them more temperature resistant. The cost issue can be addressed by making it possible to deposit device-quality material on everyday low cost plastics such as PET. This requires a production process that keeps the substrate temperature below the

substrate's deformation temperature (<100°C for many types of cheap plastics). To explore the suitability of thin film silicon for this purpose, we have performed an extensive characterization study of intrinsic and doped silicon layers at various substrate temperatures at and below 100°C.

## II. EXPERIMENTAL DETAILS

### A. Deposition

All studied layers were deposited on HF-dipped Corning 1737F glass in the ASTER [1] high vacuum multi-chamber system by VHF-PECVD at heater temperatures of 50°C, 60°C, 80°C, 100°C, 120°C and 157°C, corresponding to substrate temperatures ( $T_{\text{sub}}$ ) of 39°C, 44°C, 56°C, 67°C, 78°C and 100°C as determined from accurate temperature calibrations. The plasma excitation frequency was kept at 50 MHz and the power and pressure were kept at a constant low level. Hydrogen dilution ratios ( $r_{\text{H}} = [\text{H}_2]/[\text{SiH}_4]$ ) were varied over a broad range, such that the structure of the films at least crosses the amorphous to microcrystalline transition for all  $T_{\text{sub}}$ . All layers had a thickness of about 200 nm, except for the ones deposited at 39°C, which were made thicker (~500-1000 nm). For Fourier Transform infrared (FTIR) measurements a strip of crystalline wafer was added to all single layer depositions.

Depending on the order of deposition, thin film solar cells can be divided in two groups: p-i-n cells, where first the p-doped layer is deposited, followed by the intrinsic layer and an n-doped layer, and n-i-p cells, which are deposited in the reversed order. Since thin film silicon solar cells are always illuminated at the p-

\* correspondance: J.K.Rath@phys.uu.nl

type side, p-i-n cells are deposited on a transparent substrate and contact (TCO). The n-i-p cells can also be deposited on opaque materials. All discussed ‘standard’ p-i-n cells were deposited on (textured) Asahi U-type TCO and covered with 80 nm sputtered ZnO:Al and evaporated Ag to elongate the light path and therefore enhance the absorption in the cell by reflecting the light on the backside (Ag/ZnO:Al is called the back reflector). The ‘standard’ cell referred to in Section 3.2, had the following structure: glass/Asahi U-type SnO<sub>2</sub>/p-type a-SiC:H (200°C)/ intrinsic a-Si:H (200°C)/ n-type a-Si:H (200°C)/ZnO:Al/Ag.

### B. Characterization

The reflection and transmission spectra were recorded with two 512-pixel diode-array spectrometers in the range 400-1000 nm. To fit this optical data and obtain the refractive index and  $E_{04}$  (the photon energy that corresponds to an absorption coefficient of  $10^4$  and is a measure for the optical band gap) as a function of energy, we used the program OPTICS2, developed at Utrecht University, which solves the Maxwell equations for the coherent light in the layer and the substrate for the whole wavelength range [2].

A Digilab FTS-40 Fourier-transform spectrometer was used to collect the FTIR infrared absorption spectra. The concentration of bonded hydrogen in the film was deduced from the rocking mode of the Si-H bonds that is visible in these spectra at  $640\text{ cm}^{-1}$ .

To determine the electronic properties, dark- and photoconductivity ( $\sigma_d$  and  $\sigma_{ph}$ ) and activation energy ( $E_a$ ), two coplanar Ag contacts were evaporated on the single layers after which the conductivity was measured with a Keithley 238 Source Measure Unit, having a lower limit of  $\sim 10^{-13}\text{ A}$ . The photoconductivity measurements were performed under AM1.5 light conditions using an Oriel Solar Simulator. Activation energy measurements were done in vacuum where the samples were heated to the heater temperatures used in ASTER to avoid annealing at temperatures far above the deposition temperature.

Raman spectroscopy was used to determine the crystallinity of the material. We define the Raman crystalline ratio as  $R_c = (I_{510} + I_{520}) / (I_{480} + I_{510} + I_{520})$ , where  $I_{510}$ ,  $I_{520}$  and  $I_{480}$  are the intensities of the two crystalline and the amorphous Si-Si TO vibration lines in the Raman spectra, respectively. The spectra were recorded in a backscattering geometry, using the 514.5 nm line of a Spectra Physics Ar<sup>+</sup> ion laser, a Spex triple grating monochromator, and an EG&G CCD detector.

The IV-characteristics of the cells were measured by

means of a WACOM dual source solar simulator under AM1.5 conditions at an intensity of  $100\text{ mW/cm}^2$ .

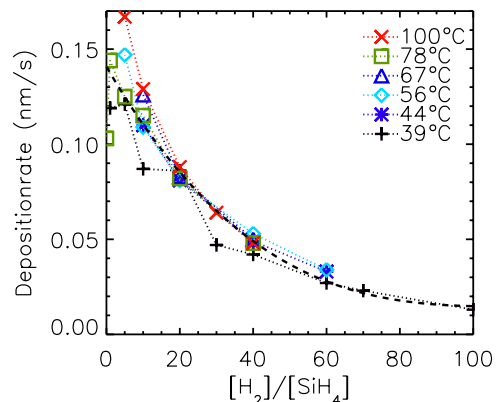


**Figure 1: Deposition rate as a function of hydrogen dilution of silane for different temperatures. The dashed line represents a second order polynomial fit to all data.**

## III. RESULTS AND DISCUSSION

### A. Temperature series

Of the three layers in an a-Si:H solar cell, the most important one to optimize is the intrinsic layer. Here, the electron-hole pairs have to be created and the free carriers have to be able to reach the front and back contacts. By measuring the structural, electronic and optical properties of different series of samples, one can decide which layers are most promising to be used in a solar cell.

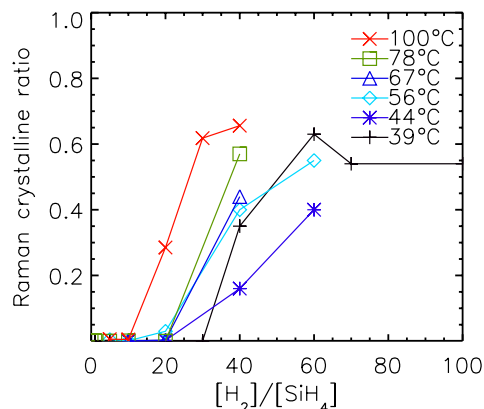


**Figure 2: The Raman crystalline ratio as a function of dilution for different temperatures. The samples that were deposited at  $T_{sub}=39^\circ\text{C}$  cannot directly be compared to the other samples, because they were thicker, which leads to a higher crystalline ratio in Raman. From X-TEM we know that the crystallinity is not homogeneous in the growth direction (see cone-shaped crystallites in Fig. 6).**

As is well known (e.g. [3],[4]), an increase in dilution ratio  $r_H$  results in a gradual transition from amorphous to microcrystalline material. We found that below 100°C the position of the (Raman) crystalline edge, i.e., the range of dilution values at which this transition takes place and where mixed phase materials are found, is very sensitive to substrate temperature (see Fig. 2). The edge shifts quickly to lower values of  $r_H$ , going from  $r_H \approx 40$  at  $T_{\text{sub}} = 39^\circ\text{C}$  to  $r_H \approx 10$  at  $T_{\text{sub}} = 100^\circ\text{C}$ , and the window in which mixed phase materials are found, becomes narrower with increasing  $T_{\text{sub}}$ . It seems that by lowering the substrate temperature below 100°C the amount of hydrogen etching, which is necessary to compensate for the surface energy loss due to the lowering of the substrate temperature, has to increase substantially to create similarly ordered material.

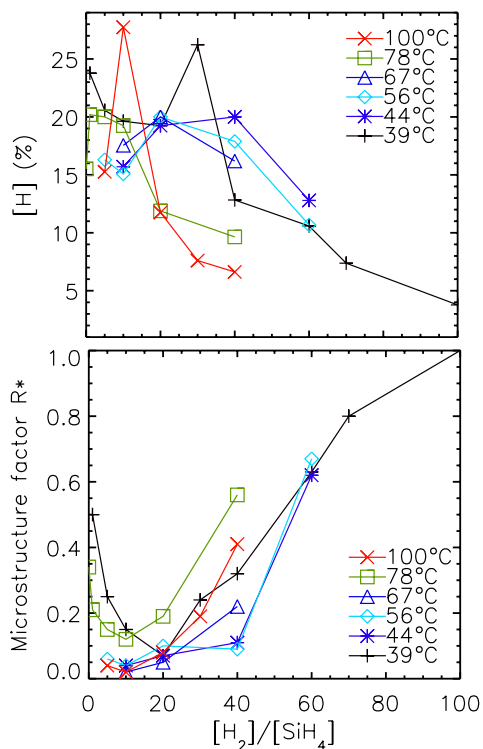


**Figure 3: Hydrogen content and microstructure factor as calculated from the rocking mode and stretching mode of FTIR measurements, respectively.**

In Fig. 3 the dilution dependence of the hydrogen content and the microstructure factor  $R^*$  are given. The microstructure factor was calculated as  $R^* = I_{2100}/(I_{2100} + I_{2000})$  where  $I_{2000}$  and  $I_{2100}$  are the intensities of the isolated Si-H and the clustered Si-H/Si-H<sub>2</sub> stretching mode peaks at respectively 2000 and 2100  $\text{cm}^{-1}$ . For all the temperatures, the hydrogen content continuously decreases as a function of dilution, as the layers become

more crystalline. Close to the crystalline edge, the hydrogen content is at its maximum. The variation of  $R^*$  behaves as the inverse of that of the refractive index (Fig. 4), confirming that  $R^*$  is inversely related to the compactness of the material. From the comparison of  $R^*$ ,  $E_{04}$ , and the refractive index (Figs. 3 and 4), a decrease of the density of the material with increasing H<sub>2</sub>-dilution is suggested for dilutions above the crystalline edge. A trend of similar slope is seen for all temperatures, suggesting a loss in density with increasing crystallinity. The densest materials are found just below the edge: at  $r_H = 20$  for  $T_{\text{sub}} = 39^\circ\text{C}$  and  $r_H = 5$  for  $T_{\text{sub}} = 100^\circ\text{C}$ .

The average value of  $E_{04}$  between  $r_H = 1$  and  $r_H = 40$  slightly increases from 1.95 eV at  $T_{\text{sub}} = 39^\circ\text{C}$  to 2.05 eV at  $T_{\text{sub}} = 100^\circ\text{C}$ , suggesting that a maximum in band gap is reached around 100°C (see [5]).

A good property to compare between layers is the photoresponse ( $\sigma_{\text{ph}}/\sigma_{\text{d}}$ ). A high  $\sigma_{\text{d}}$  in general corresponds to a disordered material and/or the presence of impurities, which reduces the minority carrier diffusion length. Therefore,  $\sigma_{\text{d}}$  should be as low as possible. On the other hand, a high  $\sigma_{\text{ph}}$  is determined by the product of the generation rate and the  $\mu\tau$ -product, which both should be as high as possible [6].

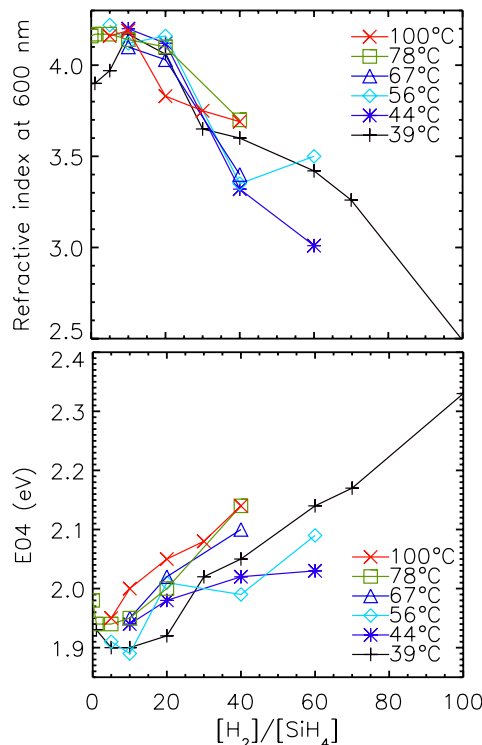


**Figure 4: Refractive index and  $E_{04}$  for different temperatures as a function of dilution.**

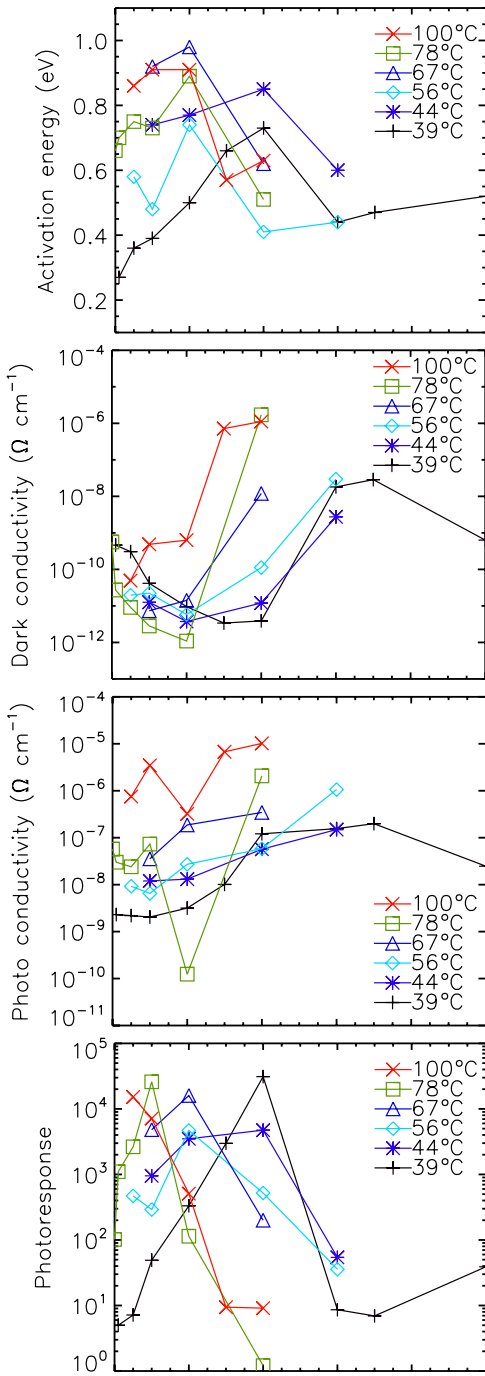


**Figure 5: Electrical properties: activation energy ( $E_a$ ),  $\sigma_{ph}$ ,  $\sigma_d$ , and their ratio plotted versus dilution.**

$\sigma_{ph}/\sigma_d$  is therefore a good indicator of the quality of these two properties and this ratio should be as high as possible (Fig. 5), a good photoresponse corresponds to a highly intrinsic layer with a low defect density. For higher temperatures the maximum in the photoresponse is found at lower dilution ratios shifting from  $r_H = 40$  ( $T_{sub} = 39^\circ\text{C}$ ) to  $r_H = 5$  ( $T_{sub} = 100^\circ\text{C}$ ), following the trend of the crystalline edge. The trend of  $E_a$  (Fig. 5) is similar to that of the photoresponse. For the optimum materials at different temperatures acceptable activation

energy values were found ( $> 0.7$  eV).

### B. Cells and materials at $39^\circ\text{C}$

A nice side effect of the slow transition from amorphous to microcrystalline material, as discussed in Section 3A, is that it makes it possible to study the transition to microcrystalline material as a function of the hydrogen to silane flow ratio in detail, because the nucleation density of crystallites becomes very sensitive to the exact value of  $r_H$ . At higher substrate temperatures the range of  $r_H$  in which one can tune the crystallinity is very narrow or even within the accuracy of mass flow controllers (MFC's), while at  $39^\circ\text{C}$  we managed to create layers with separated crystallites, so really in the middle of the transition region. Combined Cross-sectional Transmission Electron Microscope (X-TEM) and Atomic Force Microscope (AFM) measurements have led to new insights into the growth mechanism of microcrystalline silicon (see Fig. 6).

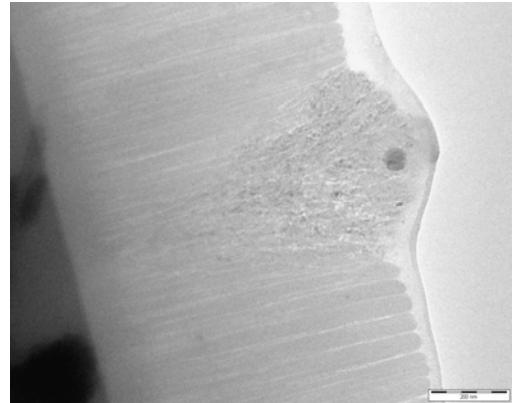


**Figure 6: TEM picture of best intrinsic layer at  $39^\circ\text{C}$ . Scale bar is 200 nm. A cone-shaped crystallite is clearly recognizable in the amorphous surroundings.**

Besides intrinsic layers also p and n-doped layers were developed at  $39^\circ\text{C}$ . Our approach was to use the recipe of the best i-layer ( $r_H = 40$ ) as a basis and vary the addition of TMB and  $\text{PH}_3$  to the source gases. The resulting layers with best electronic properties (see [7]) were tested in a solar cell by combining them with  $T_{sub} = 200^\circ\text{C}$  standard layers (Fig. 7). Both n- and p- layers made at  $T_{sub} = 39^\circ\text{C}$  are highly conductive. A series of pin solar cells was made, combining the best  $T_{sub} = 39^\circ\text{C}$  i-layer (at thicknesses ranging from 200 nm to 500 nm) with a  $T_{sub} = 200^\circ\text{C}$  p-layer and our best  $T_{sub} = 39^\circ\text{C}$  n-layer. By making the i-layer thicker, the blue response improved considerably, the conversion efficiency increasing from  $\eta = 0.50\%$  to  $\eta = 1.36\%$ . The same increase in blue response could be achieved by

applying a reverse bias of  $-1$  V to the thinnest solar cell [7], suggesting that the improvement of these cells was not caused by a ‘real’ improvement of the i-layer quality, but making it thicker led to a redistribution of the field in the front part of the cell. Replacing also the p-layer by a  $T_{\text{sub}} = 39^\circ\text{C}$  p-layer lead to a low conversion efficiency value (0.34%), though with a remarkably high yield. Further development of the complete  $T_{\text{sub}} = 39^\circ\text{C}$  solar cell is in progress, the intrinsic layer remains the most critical layer.

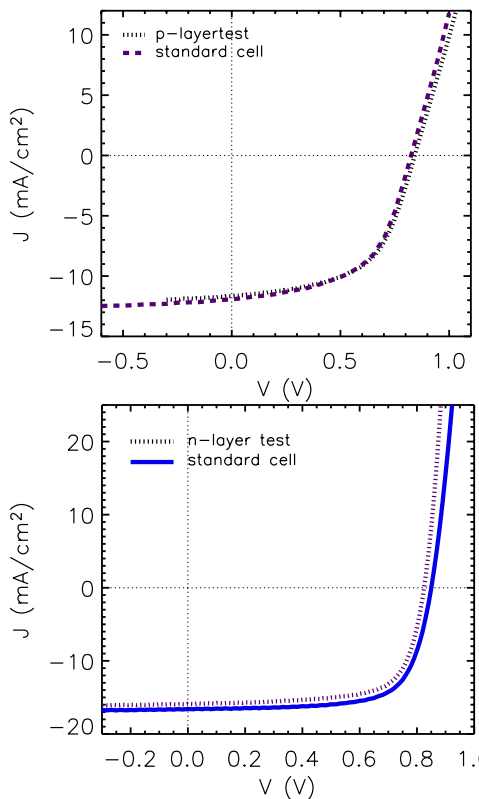


**Figure 7: Test of n-layer and p-layer made at  $T_{\text{sub}} = 39^\circ\text{C}$ . For testing the n-layer the  $200^\circ\text{C}$  n-layer of a standard pin was replaced by the  $39^\circ\text{C}$  n-layer. For testing the p-layer the p-layer of a ‘‘standard’’ nip was replaced by the  $39^\circ\text{C}$  p-layer.**

### C. Cells deposited at $100^\circ\text{C}$

From the material studies in Section A it followed that the electronically best materials within the studied temperature range were, not surprisingly, found at a temperature of  $100^\circ\text{C}$  (the best  $70^\circ\text{C}$  i-layer had a better photoresponse but a lower photoconductivity). By implementing the best i-layer made at  $T_{\text{sub}} = 100^\circ\text{C}$  in a pin structure, combined with a standard  $200^\circ\text{C}$  p-layer and a  $39^\circ\text{C}$  n-layer, an efficiency of 7.45% was reached. Because this i-layer test was successful, also doped

layers were developed at  $T_{\text{sub}} = 100^\circ\text{C}$ , again taking the i-layer recipe as a basis. Our best n-layer had  $\sigma_d = 1.5 \times 10^{-4} \Omega^{-1}\text{cm}^{-1}$  and  $E_a = 0.33$  eV and the best p-layer had  $\sigma_d = 2.9 \times 10^{-7} \Omega^{-1}\text{cm}^{-1}$ ,  $E_a = 0.51$  eV and  $E_{04} = 2.07$  eV. Combining the  $100^\circ\text{C}$  i-layer and doped layers in a pin cell on Asahi superstrates leads to cells with an average efficiency of 7.2% (best value  $\eta = 7.3\%$ ). To our knowledge this is the best result obtained so far for a cell with all silicon layers made at this low deposition temperature of  $T_{\text{sub}} = 100^\circ\text{C}$ . On ITO coated PET this recipe resulted in working cells with efficiencies of  $\sim 2.6$ - $2.9\%$ . Further development of PET-compatible ITO is presently being pursued at UU in order to obtain fully flexible solar cells on cheap plastics.

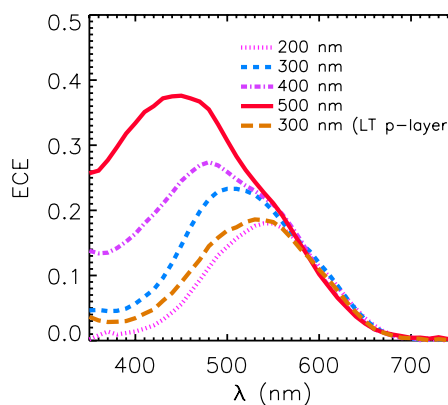


**Figure 8: Spectral response of cells from the  $39^\circ\text{C}$  i-layer thickness series without bias light.**

## IV. CONCLUSIONS

Intrinsic a-Si:H layers deposited at several different substrate temperatures below  $100^\circ\text{C}$  were tested with respect to the dependence on  $\text{H}_2$  dilution during deposition of their electronic, structural and optical properties, leading to the following insights. The deposition rate depends strongly on the dilution but very weakly on the temperature in this range. The Raman crystalline edge becomes broader and shifts to lower dilutions for lower temperatures. On or just below this edge, the electronically best materials are found, close to the maximum in hydrogen content ( $\sim 26$  at.-%). The most compact materials are always found at lower dilution values. With increasing crystallinity the material rapidly becomes more porous. Based on the  $E_{04}$  values, we infer that the optical band gap decreases towards lower temperatures in the range below  $100^\circ\text{C}$ .

Implementation of our best layers and using them as a basis for doped layers lead to good results: a working p-i-n solar cell deposited completely at  $39^\circ\text{C}$  with

promising results in test-cell configurations (1.4 %) and a high efficiency p-i-n cell made entirely at 100°C on Asahi glass/SnO<sub>2</sub> superstrates (7.3 %). This, to our knowledge, is the best a-Si:H p-i-n cell made at 100°C.

**Table I: Parameters of the solar cells made at  $T_{\text{sub}} > 39^\circ\text{C}$  discussed in the text. For the cells made at 39°C see [7]. All are averages of the best 5 values (except for the nip)**

	$\eta$ (%)	$V_{\text{oc}}$ (V)	$J_{\text{sc}}$ (mA)	FF
<b>100°C i-layer test</b>	7.5	0.86	13.2	0.66
<b>100°C pin cell</b>	7.2	0.90	13.7	0.58
<b>100°C nip cell</b>	5.0	0.85	10.7	0.56
<b>70°C i-layer test</b>	3.8	0.84	9.3	0.49
<b>100°C on PET+ITO</b>	2.9	0.89	7.5	0.43

#### ACKNOWLEDGEMENTS

We thank Jeroen Francke for the deposition of the thin layers and cells. Ronald Franken and Jochen Löffler are acknowledged for the development of the back reflectors. Eva Tois is thanked for her ITO and substrate studies.

#### REFERENCES

- [1] C.A.M. Stap, H. Meiling, G. Landweer, J. Bezemer, and W.F. van der Weg, in Proceedings of the Ninth E.C. Photovoltaic Solar Energy Conference, Freiburg, Germany (Kluwer Academic, The Netherlands, 1989) p74.
- [2] S.G. Tomlin, J. Phys. D 5 (1972), 847.
- [3] H. Fujiwara, M. Kondo, A. Matsuda, Physical Review B, 63 (2001), 115306
- [4] T. Mates et al., Journal of Non-Crystalline Solids 299-302 (2002), 767-771.
- [5] H. Meiling, PhD-thesis, Utrecht University, 1991.
- [6] M.B. von der Linden, PhD-thesis, Utrecht University, 1994.
- [7] P.C.P. Bronsveld, J.K. Rath, R.E.I. Schropp, Proceedings of the 19<sup>th</sup> EUPVSEC Paris, p. 1605 (2004)